AAS 12-269

FROZEN ORBITS FOR SCIENTIFIC MISSIONS USING ROTATING TETHERS

Hodei Urrutxua,[*] Jesús Peláez[†] and Martin Lara[‡]

We derive a semi-analytic formulation that permits to study the long-term dynamics of fast-rotating inert tethers around planetary satellites. Since space tethers are extensive bodies they generate non-keplerian gravitational forces which depend solely on their mass geometry and attitude, that can be exploited for controlling science orbits. We conclude that rotating tethers modify the geometry of frozen orbits, allowing for lower eccentricity frozen orbits for a wide range of orbital inclination, where the length of the tether becomes a new parameter that the mission analyst may use to shape frozen orbits to tighter operational constraints.

INTRODUCTION

Science orbits for missions to planetary satellites have, in general, low altitudes and near-polar inclinations so that the entire surface can be mapped, and the science requirements of the mission can be accomplished.[1,2] However, designing such an orbit can be difficult because the dynamical environment of many planetary satellites is highly perturbed due to their proximity to the central planet.[3] One such example is the Moon, on which we focus on the current study.

High-inclination orbits around the Moon are known to be unstable.[4,5,6] However, the onset of instability can be delayed by a proper orbit design, hence maximizing the orbital lifetime.[7] In this regard, the so called *frozen orbits* offer an interesting starting point for the design of science orbits,[1,8,9] since all their orbital elements, with the only exception of the mean anomaly and the longitude of the ascending node, remain constant.

The design of frozen orbits has become a key aspect of the mission analysis of lunar probes, trying to prolong their life-time as much as possible by reducing the amount of fuel dedicated to station keeping.[4,5,7] Therefore, the search for high inclination and low eccentricity frozen orbits for scientific missions has been an active field of research for the last years, and in relation to this, recent studies in the SDG-UPM research group remark that rotating space tethers can make a significant contribution to this subject.[9,10,11,12]

Because gravity is non-linear, the resultant of the gravitational force on an extensive body does not generally coincide with the force one would obtain by concentrating all the body mass at the system's center of mass. As a result, a non-keplerian perturbation term arises from the fact that the tether's mass is distributed in a finite volume, which depends solely on the tether's mass geometry

[*]PhD Student, Space Dynamics Group, Technical University of Madrid (UPM)
[†]Professor, Space Dynamics Group, Technical University of Madrid (UPM)
[‡]Scientist, Space Dynamics Group, Technical University of Madrid (UPM)
SDG-UPM Website: sdg.aero.upm.es

and attitude. This feature of space tethers allows for propellantless control of orbits, and in this particular case may even extend the domain of existence of frozen orbits.

The aim of this work is the derivation of a reliable model that adequately describes the long-term evolution of an inert rotating tether around a planetary satellite, and its application to the search for frozen orbits.

In what follows, we first introduce the concept of a rotating tethered system and its governing equations. Noticing that its dynamics takes place in different time scales, we apply successively the averaging technique to remove the short period oscillations related to the tether's rotation and the orbital motion, and hence derive averaged equations of motion that describe the long-term evolution of the tethered system. Finally, this model is applied to the search for lunar frozen orbits and the capability of rotating tethers to modify the frozen orbits geometry is discussed.

DYNAMICAL MODEL

Let us consider a tethered system formed up by two spacecraft tied one to another by a tether modeled as a long, rigid rod, according to the *dumbbell model* approximation. Both spacecraft are modeled as point masses m_1 and m_2 whereas the tether is assumed to have a homogeneous linear mass density ρ_L. The center of mass of the system, G, is then located on the tether itself, somewhere inbetween both end-masses, at distances L_1 and L_2 respectively.

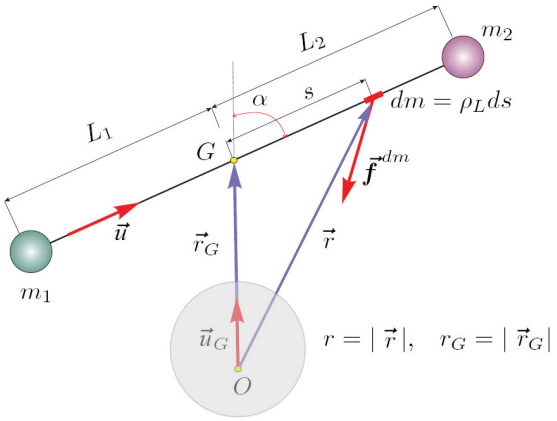

Figure 1. Geometry and kinetics of the tethered system

If we place the origin of the coordinate system O at the center of mass of the primary attracting body, we can define the position vector of the tether's center of mass as $\vec{r}_G = r_G \cdot \vec{u}_G$. Let s be a coordinate indicating the linear position of any $\mathrm{d}m$ along the tether, and $\vec{u}$ the unity vector pointing from m_1 to m_2. This allows us to define the angle α as the one formed between unity vector $\vec{u}_G$ and $\vec{u}$. Hence, as shown in Figure 1, the position of any mass element $\mathrm{d}m$ of the tether may be expressed as

$$\vec{r} = r_G \, (\vec{u}_G + \eta \cdot \vec{u}),$$

where the more convenient non-dimensional parameter $\eta = s/r_G$ is introduced, typically $\eta \ll 1$.

Notice that generally the gravitational attraction upon every single mass element $\mathrm{d}m$ of the tether does not need to be aligned with $\vec{u}$, due to the non-uniformity of the primary's gravity field. In the current paper we will consider the oblateness as the only source of non-uniformity.

The problem under consideration in this paper is the search for of lunar frozen orbits with the use of rotating space tethers. Thus, we shall condiser a tethered system orbiting around the Moon, where Moon's non-uniform gravity field and Earth's third-body perturbation are to be taken in account. Figure 1 shows the geometrical layout of the problem under study, though it must be highlighted that the current analysis remains valid for any other planetary satellite, just by conveniently switching the values of the Earth-Moon system parameters in the final expressions for the appropriate values of a different planetary system.

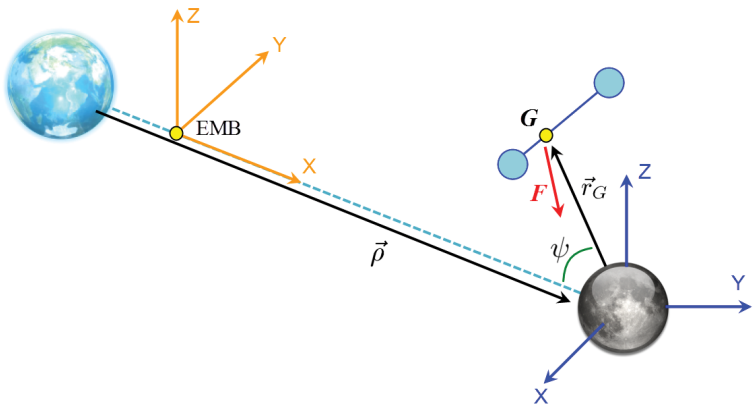

Figure 2. Sketch of the Earth-Moon-Tether system under consideration

The problem of a tethered system orbiting around a planetary satellite is a particular case of a perturbed restricted two-body problem. There are many different approaches to the two-body problem, though the large size of a tether often leaves the *Full Two-Body* approach as the most suitable one to study the dynamics of the system. In this approach both bodies, tether and primary, are considered as extensive, i.e. every mass element $\mathrm{d}m$ of one body is attracted by every $\mathrm{d}m$ of the other, leading to a double volume integral. The full two-body approach is usually avoided unless it is really neccessary, due to the inherent difficulty of the arising expressions, though when one of the two bodies is so slim as a tether, this body would very well let itself be treated as a linear geometry, turning one of the volume integrals into a linear integral.

The full two-body problem gives rise to perturbing forces due to the fact that the tether is extensive (different parts of the tether are exposed to different accelerations, giving a resultant different from that of a point mass), the fact that the primary is an extended body (the gravitational field is then non-uniform), and cross-terms from the interaction or coupling of both effects. Consequently, this approach implies a heavy mathematical formulation,[12] beyond the scope of the current manuscript. Thus, in order to keep things simple while retaining the essence of the dynamics, we shall just take into account the main contribution of both effects described above, as independent the one from the other, i.e. we will consider the dominant perturbing effect of an extensive tether around a mass point primary, and the oblateness or J_2 effect of the Moon upon a mass point tether, neglecting higher order gravitational perturbing terms. In addition to that, the third body perturbation of the Earth must also be included in the analysis, since it is a key point in the dynamnics of frozen orbits.

Translational Problem

The gravitational potential of a tether, considering the primary as a point mass, is given by

$$V = -\frac{\mu_{\leftmoon}}{r_G} \int_m \frac{\mathrm{d}m}{\sqrt{1 + 2\eta\cos\alpha + \eta^2}},$$

where the integral extends to the whole length of the tether by means of the change of variable $\mathrm{d}m = \rho_L \, r_G \, \mathrm{d}\eta$. Developing the above integral in Legendre polynomials yields

$$V = -\frac{\mu_{\leftmoon} \, m}{r_G} \sum_{n=0}^{\infty} (-1)^n \left(\frac{L_T}{r_G}\right) a_n \, P_n(\cos\alpha),$$

where L_T is the tether's length and the non-dimensioal coefficients a_n are functions of the tether's mass geometry. Further detail on the derivation is provided in References 10 and 12.

Retaining terms up to second order of L_T/r_G, we get that the gravitational perturbation upon the tether is given by

$$V \simeq -\frac{\mu_{\leftmoon} \, m}{r_G} \left(1 + \frac{L_T^2}{r_G^2} \, a_2 \, P_2(\vec{u}_G \cdot \vec{u})\right), \tag{1}$$

where $1/12 < a_2 < 1/4$. For a tether of negligible mass, the highest value $a_2 = 1/4$ corresponds to equal end masses. The other extreme value $a_2 = 1/12$ corresonds to a tether with the total mass concentrated in one of the end masses.

On the other hand, we are also interested in retaining the primary's oblateness perturbation, that we will directly add to Eq (1) in order to obtain the gravitational potential V_g, which describes the Moon-Tether gravitational interaction up to second order approximation. Hence,

$$V_g = -\frac{\mu_{\leftmoon} \, m}{r_G} \left(1 + \frac{L_T^2}{r_G^2} \, a_2 \, P_2(\vec{u}_G \cdot \vec{u}) - \frac{R_{\leftmoon}^2}{r_G^2} \, J_2 \, P_2(\vec{u}_G \cdot \vec{k})\right), \tag{2}$$

where $\vec{k}$ is a unity vector aligned with the Moon pole and $R_{\leftmoon}$ is the lunar reference radius.

Note the striking analogy between the oblateness perturbation of the primary and the non-keplerian perturbation introduced by the tether having a distributed mass. If the tether length is in the direction of $\vec{k}$, then the orbital acceleration due to the tether physical length directly substracts to the acceleration caused by the oblateness of the central body. Therefore, if we are able to maintain a non-rotating tether with this constant direction along its orbital motion, then we have an artificial way of varying the oblateness of a natural body, though it seems unlikely that the tether will evolve in this special configuration without active control.[9]

In addition to the two-body gravitational potential V_g, we also have to take into account the Earth's third-body perturbation, by means of the gravitational potential of the Earth as a third body, given by the series expansion

$$V' = -\frac{\mu_{\oplus} m}{\rho} \sum_{j=2}^{\infty} \left(\frac{r_G}{\rho}\right)^j P_j(\cos\psi),$$

where ρ is the distance from the Earth to the Moon, P_j are Legendre polynomials and ψ is the tether-Moon-Earth angle (see Figure 2). For consistency, we retain just the first term in the summation and neglect the rest, so the third-body potential of the Earth, $V_{\oplus}$, shall be

$$V_{\oplus} = -\frac{\mu_{\oplus} m}{\rho^3} \, r_G^2 \, P_2(\cos\psi) \tag{3}$$

A convenient way of describing the orbital motion of the tethered system with respect to an inertial frame located at the Moon, is by making use of the Lagrange planetary equations, which provide the time evolution of the orbital elements

$$\frac{\mathrm{d}a}{\mathrm{d}t} = \frac{2}{m\,n\,a}\,\frac{\partial \mathcal{R}}{\partial M_0} \tag{4}$$

$$\frac{\mathrm{d}e}{\mathrm{d}t} = \frac{1-e^2}{m\,n\,a^2\,e}\,\frac{\partial \mathcal{R}}{\partial M_0} + \frac{\sqrt{1-e^2}}{m\,n\,a^2\,e}\,\frac{\partial \mathcal{R}}{\partial \omega} \tag{5}$$

$$\frac{\mathrm{d}i}{\mathrm{d}t} = \frac{1}{m\,n\,a^2\,\sqrt{1-e^2}\,\sin i}\left[\frac{\partial \mathcal{R}}{\partial \Omega} - \cos i\,\frac{\partial \mathcal{R}}{\partial \omega}\right] \tag{6}$$

$$\frac{\mathrm{d}\omega}{\mathrm{d}t} = -\frac{\sqrt{1-e^2}}{m\,n\,a^2\,e}\,\frac{\partial \mathcal{R}}{\partial e} + \frac{\cot i}{m\,n\,a^2\,\sqrt{1-e^2}}\,\frac{\partial \mathcal{R}}{\partial i} \tag{7}$$

$$\frac{\mathrm{d}\Omega}{\mathrm{d}t} = \frac{-1}{m\,n\,a^2\,\sqrt{1-e^2}\,\sin i}\,\frac{\partial \mathcal{R}}{\partial i} \tag{8}$$

$$\frac{\mathrm{d}M}{\mathrm{d}t} = n - \frac{1-e^2}{m\,n\,a^2\,e}\,\frac{\partial \mathcal{R}}{\partial e} - \frac{2}{m\,n\,a}\,\frac{\partial \mathcal{R}}{\partial a} \tag{9}$$

where $\{a, e, i, \omega, \Omega, M\}$ are the classical orbital elements, n is the mean orbital motion and

$$\mathcal{R} = \mathcal{R}_g + \mathcal{R}_\oplus$$

is the perturbing potential, comprised by the terms $\mathcal{R}_g \equiv V_g + \dfrac{\mu_\leftmoon\, m}{r_G}$ and $\mathcal{R}_\oplus \equiv V_\oplus$.

Rotational Problem

The attitude dynamics is described by the time evolution of the angular momentum vector, $\vec{H}_G$. Then, the attitude equations are

$$\frac{\mathrm{d}\vec{H}_G}{\mathrm{d}t} = \vec{M} = \int_m s\,\vec{u}\wedge\,\mathrm{d}\vec{F}_m = -\frac{\mu_\leftmoon}{r_G}\,\vec{u}\wedge\vec{u}_G\int_m \frac{\eta\,\mathrm{d}m}{(\sqrt{1+2\,\eta\,\cos\alpha+\eta^2})^3},$$

where the integral extends to the whole length of the tether, and considering the primary as a mass point is in the context a fair enough approximation.

After expanding the denominator in power series of η, the torque $\vec{M}$ is integrated[12] to give

$$\vec{M} = \frac{\mu_\leftmoon\, m}{r_G}(\vec{u}\wedge\vec{u_G})\left[3\,a_2\,\frac{L_T^2}{r_G^2}\,(\vec{u}\cdot\vec{u_G}) + \mathcal{O}(L_T/r_G)^3\right]. \tag{10}$$

In the system defined by the axes of maxima inertia there is null moment of inertia around $\vec{u}$, and the inertia tensor is[9]

$$\bar{\bar{I}} = \begin{pmatrix} 0 & 0 & 0 \\ 0 & \mathcal{I} & 0 \\ 0 & 0 & \mathcal{I} \end{pmatrix},$$

where $\mathcal{I} = m\,a_2\,L_T^2$. Then, if the angular velocity of the tether, $\vec{\Omega}$, is given by

$$\vec{\Omega} = \vec{u}\wedge\frac{\mathrm{d}\vec{u}}{\mathrm{d}t} + (\vec{u}\cdot\vec{\Omega})\,\vec{u},$$

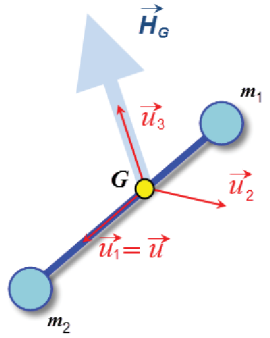

Figure 3. Sketch of tether's body frame

the angular momentum $\vec{H}_G$ can be written as

$$\vec{H}_G = \bar{\bar{I}} \cdot \vec{\Omega} = \mathcal{I}\,\vec{u} \wedge (\vec{\Omega} \wedge \vec{u}) = \mathcal{I}\,\vec{u} \wedge \frac{\mathrm{d}\vec{u}}{\mathrm{d}t}.$$

So, the angular momentum turns out to be normal to the tether. This suggests using a body-fixed reference system $Gu_1u_2u_3$ (see Figure 3), where unit vectors defining the reference frame are

$$\vec{u}_1 = \vec{u}, \qquad \vec{u}_2 = \frac{\mathrm{d}\vec{u}/\,\mathrm{d}t}{|\,\mathrm{d}\vec{u}/\,\mathrm{d}t|}, \qquad \vec{u}_3 = \vec{u}_1 \wedge \vec{u}_2$$

Then, $\vec{H}_G = \mathcal{I}\,\Omega_\perp \vec{u}_3$, where we call $\Omega_\perp \equiv |\,\mathrm{d}\vec{u}/\,\mathrm{d}t|$, and angular momentum equation may be expressed as

$$\frac{\mathrm{d}\vec{H}_G}{\mathrm{d}t} = \mathcal{I}\left(\frac{\mathrm{d}\Omega_\perp}{\mathrm{d}t}\,\vec{u}_3 + \Omega_\perp \frac{\mathrm{d}\vec{u}_3}{\mathrm{d}t}\right) = (\vec{M}\cdot\vec{u}_3)\,\vec{u}_3 + (\vec{M}\cdot\vec{u}_2)\,\vec{u}_2$$

Taking first the dot product of the later equation with $\vec{u}_3$, and then the cross product with $\vec{u}_3$ twice, along with the evolution equation of the unit vector $\vec{u}_2$, we get the set of attitude equations

$$\begin{aligned}
\frac{\mathrm{d}\vec{u}_1}{\mathrm{d}t} &= \Omega_\perp \vec{u}_2 \\
\frac{\mathrm{d}\vec{u}_3}{\mathrm{d}t} &= \frac{\vec{M}\cdot\vec{u}_2}{\Omega_\perp \mathcal{I}}\,\vec{u}_2 \\
\frac{\mathrm{d}\Omega_\perp}{\mathrm{d}t} &= \frac{\vec{M}\cdot\vec{u}_3}{\mathcal{I}}
\end{aligned}$$

with the constraints $|\vec{u}_1| = |\vec{u}_3| = 1$, $\vec{u}_1 \cdot \vec{u}_3 = 0$, that reduce the dimension of the system to two.

For describing the attitude of the tether we find convenient to use instead the *Tait-Bryan* angles, ϕ_1, ϕ_2 and ϕ_3, which are a set of Euler rotation angles in the sequence 123 or XYZ. Then, the

body frame $\{\vec{u}_1, \vec{u}_2, \vec{u}_3\}$ is expressed in the inertial frame $\{\vec{i}, \vec{j}, \vec{k}\}$ as

$$\begin{aligned}\vec{u}_1 =&(\cos\phi_2\ \cos\phi_3)\,\vec{i}_4 \\ &(\cos\phi_1\ \sin\phi_3 + \sin\phi_1\ \sin\phi_2\ \cos\phi_3)\,\vec{j}_4 \\ &(\sin\phi_1\ \sin\phi_3 - \cos\phi_1\ \sin\phi_2\ \cos\phi_3)\,\vec{k}_4\end{aligned} \tag{11}$$

$$\begin{aligned}\vec{u}_2 =&(-\cos\phi_2\ \sin\phi_3)\,\vec{i}_4 \\ &(\cos\phi_1\ \cos\phi_3 - \sin\phi_1\ \sin\phi_2\ \sin\phi_3)\,\vec{j}_4 \\ &(\sin\phi_1\ \cos\phi_3 + \cos\phi_1\ \sin\phi_2\ \sin\phi_3)\,\vec{k}_4\end{aligned} \tag{12}$$

$$\begin{aligned}\vec{u}_3 =&(\sin\phi_2)\,\vec{i}_4 \\ &(-\sin\phi_1\ \cos\phi_2)\,\vec{j}_4 \\ &(\cos\phi_1\ \cos\phi_2)\,\vec{k}_4\end{aligned} \tag{13}$$

Hence, after some algebra we find the scalar equations of the attitude dynamics[9, 10, 12]

$$\frac{\mathrm{d}\phi_1}{\mathrm{d}t} = -\frac{\vec{M}\cdot\vec{u}_2}{\Omega_\perp \mathcal{I}}\,\frac{\cos\phi_3}{\cos\phi_2} \tag{14}$$

$$\frac{\mathrm{d}\phi_2}{\mathrm{d}t} = -\frac{\vec{M}\cdot\vec{u}_2}{\Omega_\perp \mathcal{I}}\,\sin\phi_3 \tag{15}$$

$$\frac{\mathrm{d}\phi_3}{\mathrm{d}t} = \Omega_\perp + \frac{\vec{M}\cdot\vec{u}_2}{\Omega_\perp \mathcal{I}}\,\cos\phi_3\,\tan\phi_2 \tag{16}$$

$$\frac{\mathrm{d}\Omega_\perp}{\mathrm{d}t} = \frac{\vec{M}\cdot\vec{u}_3}{\mathcal{I}} \tag{17}$$

TIME SCALES AND AVERAGING

Now let us assume the tether is rotating. For such a tether, there are several different time scales involved in the dynamics. It is important to identify these scales, since different aspects of the motion of the tether are associated to one or another time scale enclosed in the problem.

The shortest time scale is the one related to the tether's self-rotation, $\Omega_\perp$. The characteristic time associated to this rotation is the inverse of $\Omega_\perp$, which allows us to introduce the non-dimensional time $\tau_1 = \Omega_\perp t$.

The next larger time scale is that associated to the tether's orbital motion around the Moon, whose characteristic time is the orbital period. Then, we may introduce the non-dimensional time $\tau = n\,t$, where n is the mean orbital motion.

Additionally, we also identify the time scale in which the Moon revolves around the Earth, which rules the third-body perturbation upon the tether. Beyond this, we still find the characteristic time in which the tether's orbit evolves, i.e. the time scale where the tether's long-term motion occurs and its orbital elements vary noticeably. The latter is the time scale where frozen orbits become meaningful. Hence, we require equations of motion that adequately keep track of the secular and long-period dynamics, while getting rid of the short-period oscillations of the motion associated

to the shortest time scales cited above. For this purpose we shall take advantage of the averaging method and apply it successively to the fast-evolving variables in our problem.

Fast Rotating Tethers

Fast rotating tethers are those that satisfy the relation $(\Omega_\perp/n) \gg 1$. For these tethers, the characteristic times related to their rotation and orbital period fulfil $\tau_1 \ll \tau$. Thus, in the time scale of the orbital period, $\tau \sim \mathcal{O}(1)$, the fast rotating tether gives several turns per orbit around the angular momentum $\vec{H}_G$. On the opposite, in the time scale of the tether's self-rotation, $\tau_1 \sim \mathcal{O}(1)$, variables whose rate of change depend on τ might be considered as *frozen* in relation to the *fast* variable τ_1, bringing the possibility of averaging the equations of motion in the fast variable ϕ_3.

To do so, it is convenient to introduce a *stroboscopic* reference system $G\vec{v}_1\vec{v}_2\vec{v}_3$, which relates to the body frame through the transformation

$$\begin{aligned}\vec{u}_1 &= +\cos\phi_3\,\vec{v}_1 + \sin\phi_3\,\vec{v}_2\\ \vec{u}_2 &= -\sin\phi_3\,\vec{v}_1 + \cos\phi_3\,\vec{v}_2\\ \vec{u}_3 &= \vec{v}_3\end{aligned}$$

For a fast rotating tether, the stroboscopic frame is attached to the instantaneous plane of rotation, and evolves in the slow time scale $\tau \sim \mathcal{O}(1)$, since $\vec{v}_1$ and $\vec{v}_2$ do not depend on ϕ_3.

Taking this on account, averaging the perturbing potential is straightforward. The third-body potential, $\mathcal{R}_\oplus$, remains unchanged, while $\mathcal{R}_g$ must be averaged since $\cos\alpha$ depends on ϕ_3. Thus, the perturbing potentials averaged in the ϕ_3 variable turn into

$$\begin{aligned}\tilde{\mathcal{R}}_g =& \frac{\mu_{\mathbb{C}}\,m}{r_G^3}\,a_2\,L_T^2\left[\frac{1}{2} - \frac{3}{4}(\vec{v}_1\cdot\vec{u}_G)^2 - \frac{3}{4}(\vec{v}_2\cdot\vec{u}_G)^2\right] + \\ &+ \frac{\mu_{\mathbb{C}}\,m}{r_G^3}\,J_2\,R_{\mathbb{C}}^2\,P_2(\vec{u}_G\cdot\vec{k}) \qquad (18)\\ \tilde{\mathcal{R}}_\oplus =& -\frac{\mu_\oplus m}{\rho^3}\,r_G^2\,P_2(\cos\psi) \qquad (19)\end{aligned}$$

Similarly, we average the attitude equations (14) to (17). In the slow time scale $\tau \sim \mathcal{O}(1)$, the rotational problem yields

$$\frac{\mathrm{d}\phi_1}{\mathrm{d}\tau} = \left(\frac{n}{\Omega_\perp}\right)\frac{a_2\,L_T}{\mathcal{I}\,\cos\phi_2}\,\frac{3}{2}\,(\vec{u}_G\cdot\vec{v}_1)\,(\vec{u}_G\cdot\vec{v}_3) \qquad (20)$$

$$\frac{\mathrm{d}\phi_2}{\mathrm{d}t\tau} = \left(\frac{n}{\Omega_\perp}\right)\frac{a_2\,L_T}{\mathcal{I}}\,\frac{3}{2}\,(\vec{u}_G\cdot\vec{v}_2)\,(\vec{u}_G\cdot\vec{v}_3) \qquad (21)$$

$$\frac{\mathrm{d}\phi_3}{\mathrm{d}\tau} = \left(\frac{\Omega_\perp}{n}\right) - \left(\frac{n}{\Omega_\perp}\right)\frac{a_2\,L_T}{\mathcal{I}}\,\frac{3}{2}\,\tan\phi_2\,(\vec{u}_G\cdot\vec{v}_1)\,(\vec{u}_G\cdot\vec{v}_3) \qquad (22)$$

$$\frac{\mathrm{d}\Omega_\perp}{\mathrm{d}\tau} = 0 \qquad (23)$$

As $n \ll \Omega_\perp$ for a fast rotating tether, we get the asymptotic solution $\mathrm{d}\phi_1/\,\mathrm{d}\tau = \mathrm{d}\phi_2/\,\mathrm{d}\tau = 0$ in the limit $\Omega_\perp \to \infty$, and the tether remains with constant attitude. This fact is of great relevance, since it implies that rotational and translational motions decouple. Hence, on the following we shall assume the tether rotates fast enough for its attitude to remain steady and not interfere with the orbital motion.

Long-Term Evolution of the System

The variation of most orbital elements is a slow process that takes place along many orbital revolutions around the primary body. If we study their time evolution on the time scale $\tau \sim \mathcal{O}(1)$ we clearly check that

$$\frac{\mathrm{d}a}{\mathrm{d}\tau} \sim \frac{\mathrm{d}e}{\mathrm{d}\tau} \sim \frac{\mathrm{d}i}{\mathrm{d}\tau} \sim \frac{\mathrm{d}\Omega}{\mathrm{d}\tau} \sim \frac{\mathrm{d}\omega}{\mathrm{d}\tau} \sim \mathcal{O}\left(\frac{1}{n}\right)^2 \qquad \text{but} \qquad \frac{\mathrm{d}M}{\mathrm{d}\tau} \sim 1 + \mathcal{O}\left(\frac{1}{n}\right)^2$$

meaning that in the natural scale in which the anomaly varies, the rest of elements remain quasi-frozen, which justifies to average the perturbing potentials (18) and (19) in the fast variable, namely an anomaly M, in order get rid of short period oscillations associated to time scales on the order of the tether's orbital period.

The averaging of a magnitude Q is really done in the time along a period, so if we wish to use another integration variable rather than time, it is neccessary that it changes linearly with time, as in the case of the mean anomaly, M. However, expressing the perturbing potentials as functions of orbital elements is more easily accomplished by using the true anomaly, through the relations

$$r_G = \frac{a\,(1-e^2)}{1+e\,\cos\nu}$$

and

$$\begin{aligned}\vec{u}_G = \quad & [\cos(\Omega)\,\cos(\omega+\nu) - \cos(i)\,\sin(\Omega)\,\sin(\omega+\nu)]\,\vec{i} + \\ & + [\sin(\Omega)\,\cos(\omega+\nu) + \cos(i)\,\cos(\Omega)\,\sin(\omega+\nu)]\,\vec{j} + \\ & + \sin(i)\,\sin(\omega+\nu)\,\vec{k}\end{aligned}$$

so, the averaging is performed according to the following relation

$$\langle Q \rangle = \frac{1}{T}\int_0^T Q\,\mathrm{d}t = \frac{1}{2\pi}\int_0^{2\pi} Q\,\mathrm{d}M = \frac{(1-e^2)^{\frac{3}{2}}}{2\pi}\int_0^{2\pi} \frac{Q\;\mathrm{d}\nu}{(1+e\,\cos\nu)^2}.$$

Without entering into the details of mathematical manipulations, which are fully covered in Reference 12, the perturbing potential (18) finally averages to

$$\hat{\mathcal{R}}_g = \quad \frac{\mu_{\mathbb{C}}\;m\,a_2\,L_T^2}{a^3\,(1-e^2)^{\frac{3}{2}}}\left[\frac{1}{2} - \frac{3}{8}(\mathbb{A}^2+\mathbb{B}^2+\mathbb{C}^2+\mathbb{D}^2)\right] + \frac{\mu_{\mathbb{C}}\;m\,J_2\,R_{\mathbb{C}}^2}{a^3\,(1-e^2)^{\frac{3}{2}}}\left[\frac{3}{4}\,\sin^2(i) - \frac{1}{2}\right] \qquad (24)$$

where the coefficients $\mathbb{A}$ to $\mathbb{D}$ are the following functions of the orbital elemenents and Tait-Bryan

rotation angles:

$$\begin{aligned}\mathbb{A} = \quad & [\cos\Omega\,\cos\omega - \cos i\,\sin\Omega\,\sin\omega]\,\cos\phi_2 + \\ & + [\sin\Omega\,\cos\omega + \cos i\,\cos\Omega\,\sin\omega]\,\sin\phi_2\,\sin\phi_1 + \\ & - \sin i\,\sin\omega\,\sin\phi_2\,\cos\phi_1\end{aligned}$$

$$\begin{aligned}\mathbb{B} = & - [\cos\Omega\,\sin\omega + \cos i\,\sin\Omega\,\cos\omega]\,\cos\phi_2 + \\ & - [\sin\Omega\,\sin\omega - \cos i\,\cos\Omega\,\cos\omega]\,\sin\phi_2\,\sin\phi_1 + \\ & - \sin i\,\cos\omega\,\sin\phi_2\,\cos\phi_1\end{aligned}$$

$$\begin{aligned}\mathbb{C} = \quad & [\sin\Omega\,\cos\omega + \cos i\,\cos\Omega\,\sin\omega]\,\cos\phi_1 + \\ & + \sin i\,\sin\omega\,\sin\phi_1\end{aligned}$$

$$\begin{aligned}\mathbb{D} = & - [\sin\Omega\,\sin\omega - \cos i\,\cos\Omega\,\cos\omega]\,\cos\phi_1 + \\ & + \sin i\,\cos\omega\,\sin\phi_1\end{aligned}$$

The Earth's perturbing potential, Eq (19), must additionally be averaged in the mean anomaly of the Moon's orbit around the Earth, since this takes place in a faster time scale than the tether's mission lifetime, which yields the expression

$$\hat{\mathcal{R}}_\oplus = -\frac{\mu_\oplus\, m}{\rho^3}\, a^2\, \frac{3}{4}\, \left[\langle \mathbb{I}^2\rangle\,(1+4\,e^2) + \langle \mathbb{J}^2\rangle\,(1-e^2) - \left(\frac{2}{3}+e^2\right)\right] \tag{25}$$

with

$$\begin{aligned}\langle \mathbb{I}^2\rangle &= \frac{1}{2}(\cos^2 i + \cos^2\omega - \cos^2 i\,\cos^2\omega)\\ \langle \mathbb{J}^2\rangle &= \frac{1}{2}(\sin^2\omega + \cos^2 i\,\cos^2\omega)\end{aligned}$$

Thus, the final averaged perturbing potential for a rotating tether in lunar orbit is

$$\hat{\mathcal{R}} = \hat{\mathcal{R}}_g + \hat{\mathcal{R}_\oplus} \tag{26}$$

where $\hat{\mathcal{R}}_g$ and $\hat{\mathcal{R}_\oplus}$ are given by Eqs. (24) and (25) respectively. Hence, entering with the partial derivatives of (26) into Lagrange equations (4) to (9) provides the set of equations that govern the long-term evolution of the tethered system.

EXTENDED FROZEN ORBITS

The reader should notice that the complexity of these governing equations is considerable due to the dependence of $\hat{\mathcal{R}}_g$ not only on the position, but on the attitude of the tether through the angles ϕ_1 and ϕ_2. So, in order to provide an insight into the effect that a rotating tether has on the orbital dynamics, it seems adequate to find some sort of simplification that reduces the complexity of these equations of motion. A convenient simplification is achieved by choosing $\phi_1 = \phi_2 = 0$, i.e.

setting the plane of rotation of the tether to be parallel to the lunar equator. Under this assumption, equations of motion drastically simplify to

$$\frac{\mathrm{d}a}{\mathrm{d}t} = \quad 0 \tag{27}$$

$$\frac{\mathrm{d}e}{\mathrm{d}t} = \quad \frac{\mu_{\oplus}}{\rho^3}\,\frac{e\,\sqrt{1-e^2}}{n}\,\frac{15}{8}\,\sin(2\,\omega)\,\sin^2(i) \tag{28}$$

$$\frac{\mathrm{d}i}{\mathrm{d}t} = -\,\frac{\mu_{\oplus}}{\rho^3}\,\frac{e^2}{n\,\sqrt{1-e^2}}\,\frac{15}{16}\,\sin(2\,\omega)\,\sin(2\,i) \tag{29}$$

$$\begin{aligned}\frac{\mathrm{d}\omega}{\mathrm{d}t} = \quad & \frac{\mu_{\mathbb{C}}}{n\,a^5\,(1-e^2)^2}\,\frac{3}{8}\,\left(5\,\cos^2 i - 1\right)\,\Big[a_2\,L_T^2 + 2\,J_2\,R_{\mathbb{C}}^2\,\Big] + \\ & + \frac{\mu_{\oplus}}{\rho^3}\,\frac{\sqrt{1-e^2}}{n}\,\frac{3}{4}\,\Big[4\,\cos^2 i + 5\,\cos^2\omega - 5\,\cos^2 i\,\cos^2\omega - 3\Big] + \\ & + \frac{\mu_{\oplus}}{\rho^3}\,\frac{\cos^2 i}{n\,\sqrt{1-e^2}}\,\frac{3}{4}\,\Big[1 + (5\,\sin^2\omega - 1)\,e^2\Big]\end{aligned} \tag{30}$$

$$\begin{aligned}\frac{\mathrm{d}\Omega}{\mathrm{d}t} = \quad & \frac{-\cos i}{n\,a^2\,\sqrt{1-e^2}}\,\frac{3}{4}\cdot \\ & \cdot\left[\frac{\mu_{\mathbb{C}}}{a^3\,(1-e^2)^{\frac{3}{2}}}\,\left(a_2\,L_T^2 + 2\,J_2\,R_{\mathbb{C}}^2\right) + \frac{\mu_{\oplus}}{\rho^3}\,a^2\,\left(1 + (5\,\sin^2\omega - 1)\,e^2\right)\right]\end{aligned} \tag{31}$$

The variation of the mean anomaly M is irrelevant for our purpose, for it does not change the shape nor the orientation of the orbit, therefore is not presented here.

This equations set is similar to those obtained by other authors,[1,3,8] that success to include the gravity perturbation due to J_2, but the novelty of our formulation is that Eqs (27) to (31) do additionally include the mechanical perturbation due to the rotating tether.

Note the semi-major axis a remains constant for the considered perturbations. This reduces the dimension of our equations system to four.

Additionally, with little algebraic manipulations this set of equations reveals that the polar component of the angular momentum, H, is preserved in the three-times-averaged problem. It is then possible to express the inclination as a function of just the eccentricity and the initial values i_0, e_0.

$$H = \sqrt{\mu_{\mathbb{C}}\,a\,(1-e^2)}\cdot\cos(i) = \sqrt{\mu_{\mathbb{C}}\,a\,(1-e_0^2)}\cdot\cos(i_0)$$

Also note that eq. (31) evidences that a rotating tether increases the regression of nodes, since its contribution directly sums that of the primary's oblateness. This property of fast rotating tethers had already been discovered in recent researches by our group. In fact, Reference 9 explains that a fast rotating tether in a plane parallel to the equatorial plane of the attracting body reinforces the oblateness effect produced by the attracting body. Hence, looking at the analogy between the tether

perturbation and the J_2 perturbation, we observe that a tether length

$$L_T = R_{\leftmoon} \sqrt{\frac{2\,J_2}{a_2}} \simeq 70\,\mathrm{km}$$

would give rise to a perturbation equal in magnitude to that of the lunar oblateness, therefore obtaining an effect analog to doubling the actual lunar J_2 coefficient.

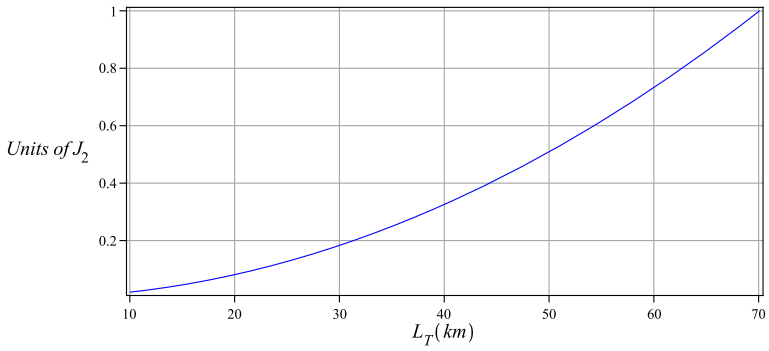

Figure 4. Artificial effect of the tether's length on the oblateness coefficient.

This result is quite relevant since it is well known that the oblateness perturbation may have a beneficial effect in general scenarios in which other perturbations tend to destabilize the dynamics. Thus, by the simple expedient of lengthening an inert tether, we might mitigate instabilities induced by the dynamics.

This possibility of artificially increasing the effect of the oblateness of a celestial body is of particular interest for the Moon, whose natural oblateness is not as big as for the Earth and consequently the J_2 zonal harmonic does not dominate clearly over all other harmonics.[13, 14]

Note that eqs. (28) to (30) are independent from the motion of the longitude of the ascending node, Ω, so we can ignore eq. (31) when determining the frozen orbit solutions. When in a frozen orbit, its value will simply circulate. Thus, frozen orbits are obtained by definition as the stationary solutions

$$\frac{\mathrm{d}e}{\mathrm{d}t} = \frac{\mathrm{d}i}{\mathrm{d}t} = \frac{\mathrm{d}\omega}{\mathrm{d}t} = 0$$

leading to a set of non-linear algebraic equations on the variables a, e, i and ω. If we first consider equations (28) and (29) and set them equal to zero, we find the possible solutions

$$e = 0, \qquad i = 0, \qquad \omega = 0 \;\text{ or }\; \pi, \qquad \text{and} \qquad \omega = \pm\frac{\pi}{2}$$

Entering each of them (which fixes one of the four variables) into equation (30) results in an implicit equation of three variables that provides the locus of the variables such that the resulting orbit is frozen. In other words, each of the conditions above leads to a different family of frozen orbits, each with different properties.

The condition $i = 0$ leads to the only solution $e = 1$, leaving ω undetermined. Since in this analysis, we are only considering closed orbits, this singular solution will not be treated. The

condition $e = 0$ is not valid either, since the argument of periapsis would not be properly defined with this set of orbital elements, so the condition $e = 0$ is discarded as well.

As mentioned before, the Moon is less flattened than Earth in the way that its oblateness coefficient does not play a dominant role in a gravitational field in which its lumpy character confers similar importance to a high number of harmonics. This means that retaining only J_2 is insufficient to properly describe the dynamics of lunar probes, which implies that any serious study should consider at least the first 20 zonals or preferably more.

As a consequence, we include the perturbing potential of further zonals harmonics, given by

$$\hat{\mathcal{R}}_{J_n} = -\frac{\mu_{\mathbb{C}}}{r_G} \sum_{n\geq 2} \left(\frac{R_{\mathbb{C}}}{r_G}\right)^n J_n \sum_{p=0}^{n} F_{n,0,p}(i)\, G_{n,p,(2p-n)}(e) \begin{cases} \cos[(n-2p)\,\omega] & (l-2p) \text{ even} \\ \sin[(n-2p)\,\omega] & (l-2p) \text{ odd} \end{cases}$$

where $F(i)$ and $G(e)$ are Kaula's inclination and eccentricity functions, respectively, into our dynamical model. Two major consequences occur when adding more zonals: on the one hand, frozen orbits come to exist in a wider range of inclinations and with different values of the eccentricity, and on the other hand, frozen orbits happen to exist also for values of ω different from $\omega = \pm\pi/2$ or $\omega = 0$, enriching the atlas of frozen orbits.

More particularly, the value $\omega = \pi/2$ automatically satisfies Equations (28) and (29) for any arbitrary number or zonal harmonics, so the problem reduces to finding the roots of Eq. (30), that becomes an implicit function of the eccentricity and the inclination. This fact allows to plot frozen orbits in inclination-eccentricity diagrams. Figures 5 and 6 show a few of these diagrams for different altitudes, comparing the original frozen orbits with the *extended* ones that could be achieved by using a rotating tether of 40 or 70 kilometers. As clearly shown, the rotating tether allows for lower eccentricity frozen orbits, which may mean a remarkable benefit for scientific missions.

Thus, frozen orbits are defined for non-tethered satellites by a combination of the four orbital elements a, e, i and ω. For rotating tethered satellites instead, the length of the tether, L_T, is a free parameter that directly affects the existence of frozen orbits.

Furthermore, the capability of the tether to modify the locus of frozen orbits permits to literally *build* or *design* a frozen orbit that best fulfils our mission requirements, just by finding an optimal combination of a, e, i, ω and L_T. Hence, the tether includes a fifth design parameter on which frozen orbits depend, so the tether length can be seen as an extra degree of freedom that the mission analyst could use to design a new frozen orbit or shape an existing one.

CONCLUSIONS

Througout the current paper we have developed a formulation that allows for the study of the long term evolution of a rotating tethered system around a planetary satellite, and apply it to the search for lunar frozen orbits.

By the simple observation of the three-times averaged equations of the motion we were able to reproduce recently discovered orbit stabilization capabilities that arise from the simple fact of lengthening an inert tether, which allows to mitigate instabilities induced by the orbital dynamics in highly perturbed scenarios by artificially increasing the effect of the oblateness of a celestial body, hence bringing new possibilities to the exploration of planetary satellites.

We also shed some light onto the potential capability of rotating tethers to modify the frozen orbits geometry, allowing to achieve lower eccentricity frozen orbits. In fact, the length of the tether

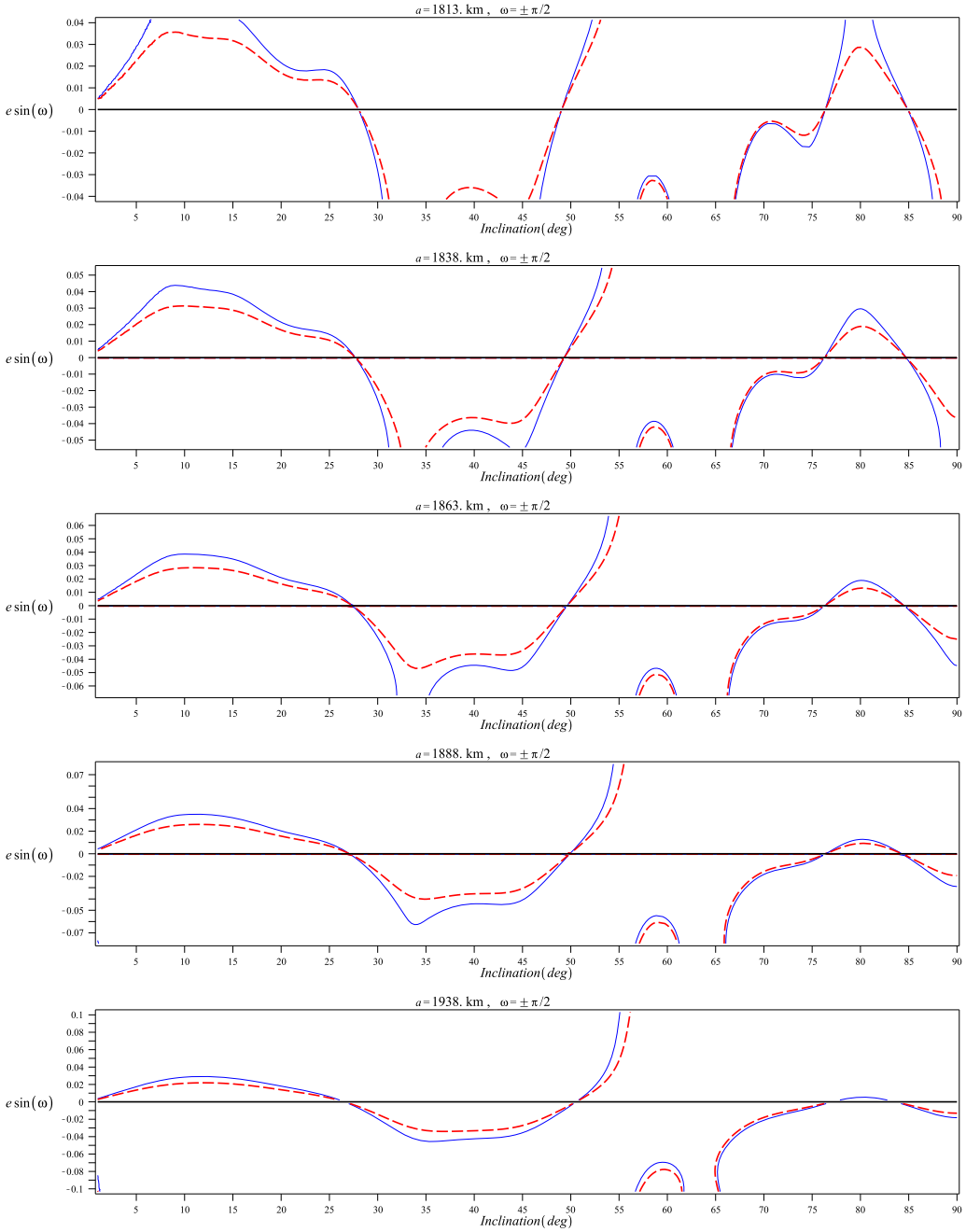

Figure 5. Inclination-eccentricity diagrams of low lunar frozen orbits, taking first 40 zonals. Full line: natural dynamics. Dashed line: dynamics for a fast rotating tether parallel to the Moon's equatorial plane, with $L_T = 40\,\mathrm{km}$ and $a_2 = 1/4$.

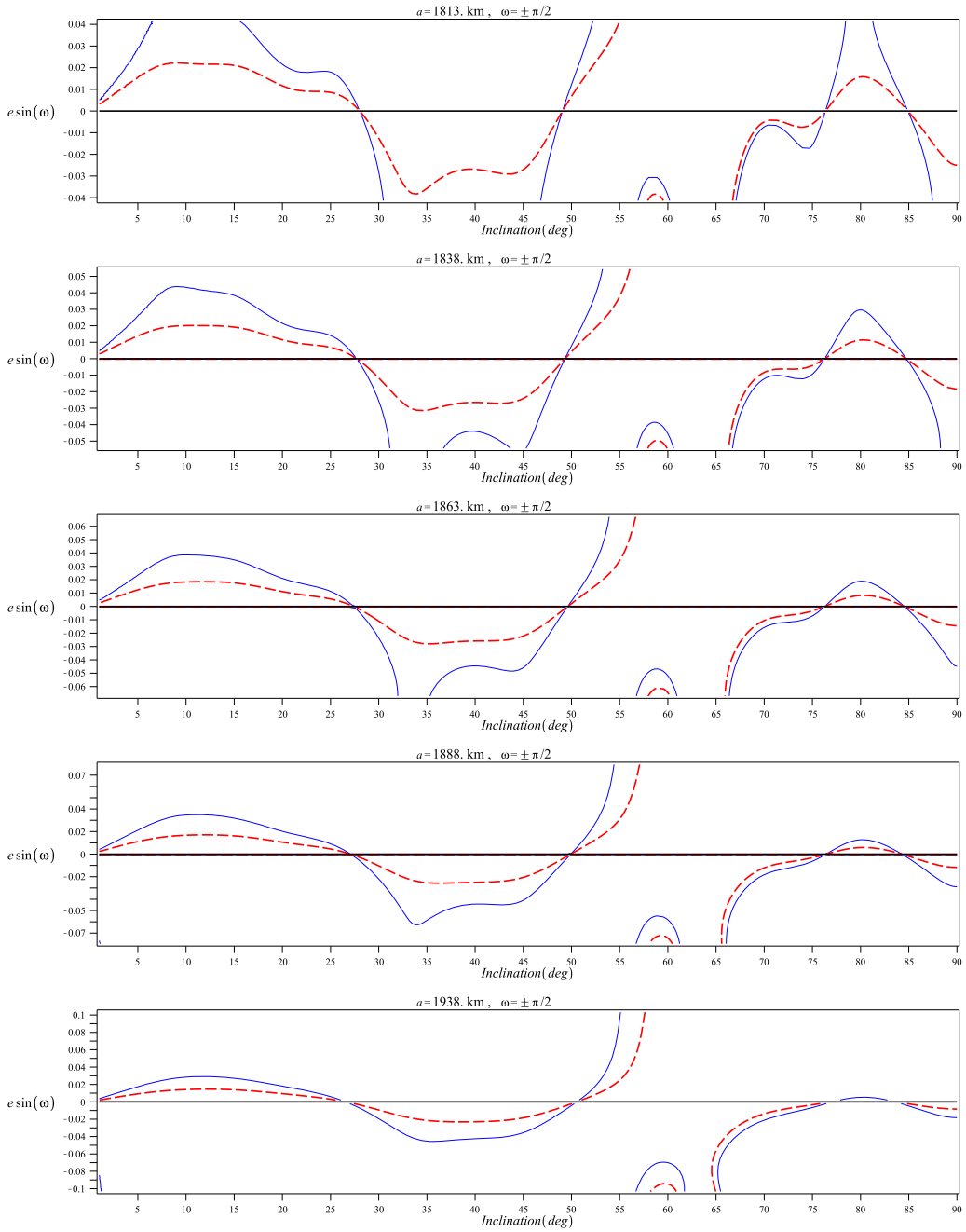

Figure 6. Inclination-eccentricity diagrams of low lunar frozen orbits, taking first 40 zonals. Full line: natural dynamics. Dashed line: dynamics for a fast rotating tether parallel to the Moon's equatorial plane, with $L_T = 70\,\mathrm{km}$ and $a_2 = 1/4$.

becomes a new parameter in the design of frozen orbits, giving the mission analyst an extra degree of freedom that allows for an optimal mission design, by properly selecting the best combination of the orbital elements that leads to the desired frozen orbit.

ACKNOWLEDGMENT

The content of the current article is based on a MSc Project (Reference 12) that was proposed and supervised by Prof. Jesús Peláez (*Universidad Politécnica de Madrid*) and scientist Martín Lara (*Real Observatorio de la Armada*), whose work was conducted in the framework of the research project "Dynamic Simulation of Complex Space Systems", supported by the Dirección General de Investigación of the Spanish Ministry of Education and Science through contract AYA2010-18796.

We would also like to thank the Technical University of Madrid (UPM) for supporting Hodei Urrutxua in the endeavour of his Ph.D. research.

REFERENCES

[1] M. E. Paskowitz and D. J. Scheeres, "Orbit Mechanics About Planetary Satellites - Dynamics of Planetary Satellite Orbiters," *American Astronautical Society*, Vol. 224, 2004, pp. 1–17.

[2] M. Lara and R. Russell, "Computation of a Science Orbit About Europa," *Journal of Guidance, Control, and Dynamics*, Vol. 30, Jan. 2007, pp. 259–263, 10.2514/1.22493.

[3] M. Paskowitz Possner and D. J. Scheeres, "Control of Science Orbits About Planetary Satellites," *Journal of Guidance, Control, and Dynamics*, Vol. 32, Jan. 2009, pp. 223–231, 10.2514/1.36220.

[4] K. W. Meyer, J. J. Buglia, and P. N. Desai, "Lifetimes of Lunar Satellite Orbits," Technical Paper 3394, NASA, March 1994.

[5] Z. Kenežević and A. Milani, "Orbit maintenance of a lunar polar orbiter," *Planetary Space Sciences*, Vol. 46, 1998, pp. 1605–1611.

[6] V. Béletski, *Essais sur le mouvement des corps cosmiques*. MIR, 1997.

[7] M. Lara, "Design of Long-Lifetime Lunar Orbits: A Hybrid Approach," *GLUC*, Vol. 2.2.2, 2010, pp. 1–15.

[8] M. Lara and J. F. Palacián, "Hill Problem Analytical Theory to the Order Four: Application to the Computation of Frozen Orbits around Planetary Satellites," *Mathematical Problems in Engineering*, Vol. 2009, 2009, pp. 1–19, 10.1155/2009/753653.

[9] M. Lara and J. Peláez, "Modifying the Atlas of Low Lunar Orbits Using Inert Tethers," *GLUC*, Vol. 2.2.7, 2010, pp. 1–7.

[10] J. Peláez, M. Sanjurjo, F. R. Lucas, M. Lara, E. C. Lorenzini, D. Curreli, and D. J. Scheeres, "Dynamics and Stability of Tethered Satellites at Lagrangian Points," Ariadna Study 07/4201, European Space Agency, 2007.

[11] J. Peláez, M. Lara, M. Sanjurjo Rivo, and D. J. Scheeres, "Periodic Orbits of a Hill-Tether Problem Originated from Collinear Points," *Journal of Guidance, Control, and Dynamics*, Vol. 35, No. 1, 2012, pp. 222–233.

[12] H. Urrutxua Cereijo, "Use of Rotating Space Tethers in the Exploration of Celestial Bodies," master thesis, ETSI Aeronáuticos, October 2010.

[13] R. B. Roncoli, "Lunar Constants and Models Document," Tech. Rep. JPL D-32296, Jet Propulsion Laboratory, September 23 2005.

[14] A. S. Konopliv, S. W. Asmar, E. Carranza, W. L. Sjogren, and D. N. Yuan, "Recent Gravity Models as a Results of the Lunar Prospector Mission," *Icarus*, Vol. 150, 2001, pp. 1–18.